Role of the Proposed Pore-Forming Segment of the Ca^{2+} Release Channel (Ryanodine Receptor) in Ryanodine Interaction*

S. R. Wayne Chen, Pin Li, Mingcai Zhao, Xiaoli Li, and Lin Zhang

Cardiovascular Research Group, Department of Physiology and Biophysics, and Department of Biochemistry and Molecular Biology, University of Calgary, Calgary, Alberta T2N 4N1, Canada

ABSTRACT In earlier studies we showed that point mutations introduced into the proposed pore-forming segment, GVRAGGGIGD (amino acids 4820–4829), of the mouse cardiac ryanodine receptor reduced or abolished high affinity [^{3}H]ryanodine binding. Here we investigate the effects of these mutations on the affinity and dissociation properties of [^{3}H]ryanodine binding and on ryanodine modification of the ryanodine receptor channel at the single channel and whole cell levels. Scatchard analysis and dissociation studies reveal that mutation G4824A decreases the equilibrium dissociation constant (K_d) and the dissociation rate constant (k_{off}), whereas mutations G4828A and D4829A increase the K_d and k_{off} values. The effect of ryanodine on single G4828A and D4829A mutant channels is reversible on the time scale of single channel experiments, in contrast to the irreversible effect of ryanodine on single wild-type channels. Ryanodine alone is able to induce a large and sustained Ca^{2+} release in HEK293 cells transfected with the R4822A or G4825A mutant cDNA at the resting cytoplasmic Ca^{2+} but causes little or no Ca^{2+} release in cells transfected with the wild-type cDNA. Mutation G4826C diminishes the functional effect of ryanodine on Ca^{2+} release but spares caffeine-induced Ca^{2+} release in HEK293 cells. Co-expression of the wild-type and G4826C mutant proteins produces single channels that interact with ryanodine reversibly and display altered conductance and ryanodine response. These results are consistent with the view that the proposed pore-forming segment is a critical determinant of ryanodine interaction. A putative model of ryanodine-ryanodine receptor interaction is proposed.

INTRODUCTION

Ryanodine, a plant alkaloid, is a specific modulator of Ca^{2+} release channels (ryanodine receptors) (RyRs), which mediate the release of Ca^{2+} from sarco(endo)plasmic reticulum and play an essential role in various fundamental processes (Berridge, 1993; Clapham, 1995; Coronado et al., 1994; Franzini-Armstrong and Protasi, 1997; Meissner, 1994; Ogawa, 1994; Sutko et al., 1997). The remarkable specificity and high affinity of ryanodine binding has made the identification, purification, and cloning of RyRs possible. Ryanodine binding has also been widely used in the functional characterization of RyRs (Coronado et al., 1994; Franzini-Armstrong and Protasi, 1997; Meissner, 1994; Ogawa, 1994). However, despite the extensive use and the pivotal role of ryanodine in the investigation of RyR function and regulation and in intracellular Ca^{2+} signaling, the structural basis for ryanodine interaction remains largely undefined.

Functional and biophysical studies have provided a great deal of information about the mechanism of interaction between ryanodine and its receptor (Coronado et al., 1994; Franzini-Armstrong and Protasi, 1997; Meissner, 1994; Ogawa, 1994; Sutko et al., 1997; Williams et al., 2001). It has been demonstrated that the ryanodine binding site is accessible only from the cytoplasmic side of the RyR channel and that ryanodine binds only to the open state of the channel (Tanna et al., 1998). Upon binding, ryanodine, at low concentrations, shifts the channel into a state of high open probability and reduced conductance, leading to channel activation. At higher concentrations, it closes the channel (Lai et al., 1989; McGrew et al., 1989; Pessah and Zimanyi, 1991). The reduction in single channel conductance upon ryanodine binding is believed to result from alterations in ion binding and ion handling (Lindsay et al., 1994). Recently, new insights into the mechanism of ryanodine action have been obtained by studying interactions between RyR and a number of ryanodine analogues (Welch et al., 1994, 1996, 1997). These studies have revealed that the pyrrole group of the ryanodine molecule is the most important structural locus for high affinity ryanodine binding (Welch et al., 1996, 1997). The binding affinity and the conductance of the ryanoid-modified state vary among ryanodine derivatives, some of which exhibit reversible effect on single RyR channel function (Tanna et al., 1998; Tinker et al., 1996; Welch et al., 1996, 1997). Further analyses of some reversible ryanoids have demonstrated that ryanoid binding is influenced by transmembrane voltage (Tanna et al., 1998, 2000; Tinker et al., 1996). Based on the results of these functional studies and comparative molecular field analysis of ryanodine derivatives, it has been proposed that the ryanodine binding site is likely to locate within the large vestibule of the conduction pathway of the RyR channel (Tanna et al., 1998, 2000; Tinker et al., 1996).

In accordance with this proposition, earlier biochemical studies localized both the high and low affinity ryanodine binding sites to a 76-kDa COOH-terminal tryptic fragment

Submitted October 20, 2001, and accepted for publication February 11, 2002.

S. R. Wayne Chen is a Senior Scholar of the Alberta Heritage Foundation for Medical Research.

Address reprint requests to Department of Physiology and Biophysics, University of Calgary, 3330 Hospital Drive NW, Calgary, Alberta T2N 4N1, Canada. Tel.: 403-220-4235; Fax: 403-283-4841; E-mail: swchen@ucalgary.ca.

0006-3495/02/05/2436/12 $2.00

of the skeletal muscle ryanodine receptor (RyR1) (Callaway et al., 1994; Witcher et al., 1994). Recent functional expression studies revealed that the COOH-terminal fragment (~1000 amino acids) of RyR1 was sufficient to form a Ca^{2+}- and ryanodine-sensitive Ca^{2+} release channel (Bhat et al., 1997), indicating that the COOH terminal fragment contains the functional ryanodine interacting site. However, specific regions or amino acid residues within this 76-kDa COOH terminal fragment that are important for ryanodine binding have yet to be identified. Recently, we have shown that a single substitution of alanine for glycine at position 4824 in the mouse cardiac ryanodine receptor (RyR2) decreased the single channel conductance by 97% (Zhao et al., 1999). We have hypothesized that a highly conserved region, GVRAGGGIGD^{4829}, constitutes the pore-forming segment of RyR. More recently, the corresponding regions in RyR1 and in rabbit RyR2 have also been proposed to contribute to the formation of the ion-conducting pathway of the RyR channel (Du et al., 2001; Gao et al., 2000). Mutations within or near this proposed pore-forming segment reduced or abolished [^{3}H]ryanodine binding (Du et al., 2001; Gao et al., 2000; Zhao et al., 1999).

To further investigate the role of the proposed pore-forming segment of RyR in ryanodine interaction, we investigated in the present study the effects of mutations in this segment on the affinity and dissociation properties of [^{3}H]ryanodine binding and on ryanodine modification of the RyR channel at the single channel and whole cell levels. We demonstrate that mutations in the proposed pore-forming segment alter the affinity and dissociation properties of [^{3}H]ryanodine binding, the reversibility and characteristics of ryanodine modification, and the conductance, gating, and stability of the ryanodine-modified state. Furthermore, we show that mutation G4826C within this segment eliminates the effect of ryanodine without abolishing caffeine response. These observations suggest that the proposed pore-forming segment of RyR is an essential determinant of ryanodine interaction. Part of this work has been presented in an abstract form (Chen et al., 2000).

MATERIALS AND METHODS

Materials

Ryanodine was obtained from Calbiochem. [^{3}H]ryanodine was from NEN Life Science Products (Boston, MA). Brain phosphatidylserine was from Avanti Polar Lipid. Synthetic 1,2-dioleoyl-*sn*-glycerol-3-phosphoethanolamine and 1-palmitoyl-2-oleoyl-*sn*-glycero-3-phosphocholine were from Northern Lipids. 3-[(3-Cholamidopropyl)-dimethylammonio]-1-propane sulfonate and other reagents were purchased from Sigma (St. Louis, MO).

Site-directed mutagenesis

Point mutations were introduced into the proposed pore-forming segment of the mouse cardiac ryanodine receptor by the overlapping extension method (Ho et al., 1989) using the polymerase chain reaction as described previously (Zhao et al., 1999). Transfection of HEK293 cells was carried out using the Ca^{2+} phosphate precipitation method.

Preparations of cell lysates

HEK293 cells grown for 24 to 26 h after transfection were washed three times with phosphate-buffered saline (137 mM NaCl, 8 mM Na_2HPO_4, 1.5 mM KH_2PO_4, 2.7 mM KCl) plus 2.5 mM EDTA and harvested in the same solution by centrifugation. Cells from 10 10-cm tissue culture dishes were solubilized in a 2-mL lysis buffer containing 25 mM Tris, 50 mM Hepes (pH 7.4), 137 mM NaCl, 1% 3-[(3-cholamidopropyl)-dimethylammonio]-1-propane sulfonate, 0.5% egg phosphatidylcholine, 2.5 mM dithiothreitol, and a protease inhibitor mix (1 mM benzamidine, 2 μg/mL leupeptin, 2 μg/mL pepstatin A, 2 μg/mL aprotinin, and 0.5 mM phenylmethylsulfonyl fluoride) on ice for 1 h. Cell lysates were obtained after removing the unsolubilized materials by centrifugation.

[^{3}H]Ryanodine binding

Equilibrium [^{3}H]ryanodine binding to cell lysates was carried out as described previously (Li and Chen, 2001) with some modifications. [^{3}H]ryanodine binding was carried out in a total volume of 300 μL of binding solution containing 30 μL of cell lysate (3.5–5.9 mg/mL), 500 mM KCl, 25 mM Tris, 50 mM Hepes, pH 7.4, 0.5 mM EGTA, 0.7 mM $CaCl_2$, 0.1 to 100 nM [^{3}H]ryanodine, and the protease inhibitor mix at 37°C for 2 h. The binding mix was diluted with 5 mL ice-cold washing buffer containing 25 mM Tris, pH 8.0, and 250 mM KCl and was immediately filtered through Whatman GF/B filters presoaked with 1% polyethylenimine. The filters were washed and the radioactivities associated with the filters were determined by liquid scintillation counting. Nonspecific binding was determined by measuring [^{3}H]ryanodine binding in the presence of 20 μM unlabeled ryanodine. All binding assays were done in duplicate. To determine the dissociation rate constants, [^{3}H]ryanodine binding was carried out in a binding buffer containing 500 mM KCl, 25 mM Tris, 50 mM Hepes, pH 7.4, 2 mM caffeine, 0.2 mM EGTA, and 0.25 mM $CaCl_2$. The binding mixture after 2 h incubation at 37°C was diluted 10 times in a dissociation buffer containing 25 mM Tris, pH 7.5, 250 mM KCl, 5 mM EGTA, and 5 mM $MgCl_2$ and incubated at room temperature for 0 to 30 min. The amount of [^{3}H]ryanodine remained bound was determined as described above. Statistical comparisons were carried out by using the unpaired Student's *t*-test.

Ca^{2+} release measurements and single channel recordings

Free cytosolic Ca^{2+} concentration in transfected HEK293 cells was measured with the fluorescence Ca^{2+} indicator dye fluo-3-AM as described previously (Li and Chen, 2001). Recombinant mouse cardiac ryanodine receptor proteins were purified from whole cell lysate by sucrose density gradient centrifugation and were used for single channel recordings as described previously (Li and Chen, 2001). Free Ca^{2+} concentrations were calculated using the computer program of Fabiato and Fabiato (1979).

RESULTS

Mutations in the proposed pore-forming segment alter the affinity and dissociation properties of [^{3}H]ryanodine binding

To further understand the effects of mutations in the proposed pore-forming segment (Fig. 1 *a*) on ryanodine interaction, we determined the affinity of [^{3}H]ryanodine binding

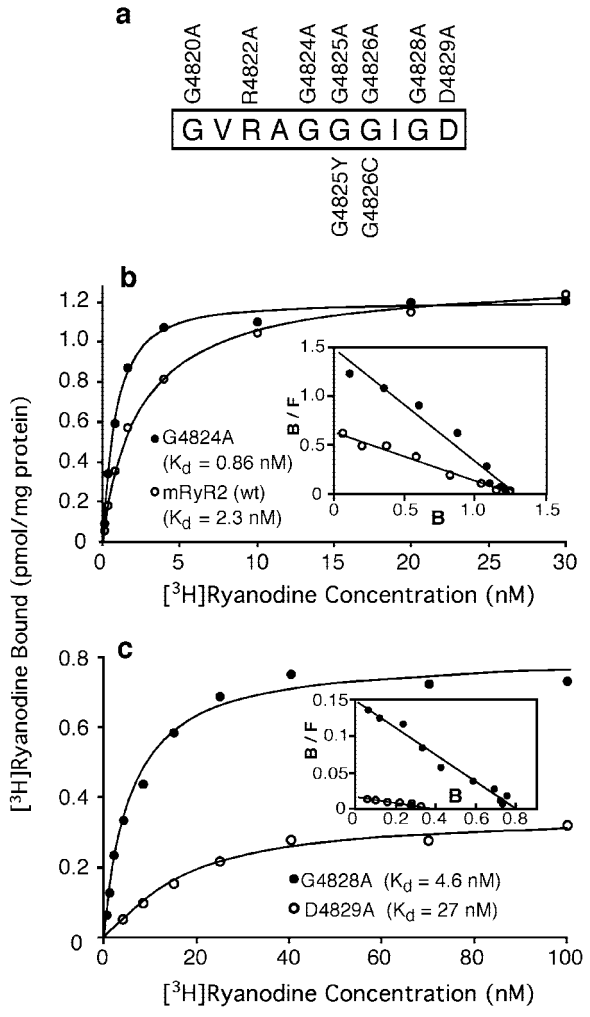

FIGURE 1 Mutations in the proposed pore-forming segment alter the affinity of [^{3}H]ryanodine binding. (*a*) The amino acid sequence in single letter codes of the proposed pore-forming segment of the mouse RyR2 (*boxed*) and the mutants used in the present study. Mutations G4820A, R4822A, G4824A, G4825A, G4826A, G4828A, and D4829A were made previously (Zhao et al., 1999, whereas mutations G4825Y and G4826C were made in the present study). [^{3}H]ryanodine binding to cell lysates prepared from HEK293 cells transfected with wt or mutant RyR2 cDNA was carried out as described in the Materials and Methods. (*b*) [^{3}H]ryanodine binding to cell lysate of wild-type (wt) (○) or G4824A mutant (●). (*c*) [^{3}H]ryanodine binding to cell lysate of mutant G4828A (●) or mutant D4829A (○). Insets in *b* and *c* are Scatchard plots. Data shown are from representative experiments each repeated 3 to 4 times. Binding data for mRyR2 (wt) were taken from a previous study (Li and Chen, 2001) for direct comparison.

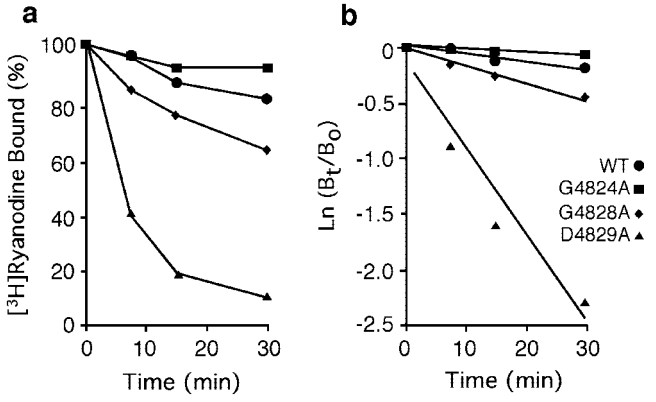

FIGURE 2 Mutations in the proposed pore-forming segment affect the dissociation properties of [^{3}H]ryanodine binding. (*a*) Amount of [^{3}H]ryanodine remained bound to wt, G4824A, G4828A, and D4829A after incubating in the diluting buffer for 0 to 30 min. (*b*) Plot of ln(Bt/Bo) versus time. Bt is the specific binding at time *t*, and Bo is the specific binding at time 0. The k_{off} values were calculated according to the equation $k_{off}\,t = \ln(Bt/Bo)$. Data shown are from a representative experiment that has been repeated three to five times.

to wild-type (wt) and to mutants G4824A, G4828A, and D4829A. Scatchard analysis revealed that mutations in this region could either increase or decrease the affinity of [^{3}H]ryanodine binding (Fig. 1, *b* and *c*). Mutation G4824A decreased the equilibrium dissociation constant (K_d) value from 2.3 ± 0.63 nM (means ± SE, $n = 4$) of the wt to 0.86 ± 0.14 nM ($n = 4$), hence increasing the binding affinity by approximately threefold (significantly different, $p < 0.005$). On the other hand, mutations G4828A and D4829A increased the K_d values to 4.6 ± 0.88 ($n = 4$) and 27 ± 3.5 nM ($n = 3$), thus decreasing the binding affinity by approximately twofold ($p < 0.005$) and 12-fold ($p < 0.0001$), respectively. Reduced levels of maximal [^{3}H]ryanodine binding (B_{max}) were observed in mutant G4828A and D4829A cell lysates as compared with that in the wt cell lysate. The B_{max} values for mutant G4828A and mutant D4829A are 0.84 ± 0.26 and 0.32 ± 0.16 pmol/mg, respectively. The B_{max} value for mutant G4824A is 1.14 ± 0.30 pmol/mg, similar to that of the wt (1.24 ± 0.26 pmol/mg).

It has been shown that the rate of association of ryanodine with RyR is linearly dependent on the open probability (Po) of the RyR channel, whereas the rate of dissociation is independent of Po (Tanna et al., 1998). To examine the effect of these mutations on [^{3}H]ryanodine binding without the influence of channel Po, we determined the dissociation kinetics of [^{3}H]ryanodine binding to mutant and wt proteins. Bound [^{3}H]ryanodine was found to dissociate from mutants G4828A and D4829A at a faster rate than that of the wt, whereas mutant G4824A exhibited a slower rate of dissociation (Fig. 2, *a* and *b*). The dissociation rate constants (k_{off}) (Weiland and Molinoff, 1981) for mutants G4828A and D4829A are 0.024 ± 0.011 min^{-1} ($n = 5$), and 0.081 ± 0.044 min^{-1} ($n = 5$), approximately fourfold ($p < 0.01$) and 13-fold ($p < 0.005$) greater than that of wt (0.0062 ± 0.0019 min^{-1}, $n = 5$), respectively. On the other hand, k_{off} for mutant G4824A (0.0021 ± 0.0005 min^{-1}, $n = 3$) is approximately threefold ($p < 0.02$) lower than that of the wt. The extents of these changes in k_{off} values are comparable with those in K_d values, suggesting that mutations in the proposed pore-forming segment can alter the affinity of

[^{3}H]ryanodine binding by either decreasing or increasing the dissociation rate.

Reversible effect of ryanodine on single D4829A and G4828A mutant channels

Recently, several ryanodine derivatives have been reported to exert reversible effect on single cardiac RyR channels (Tanna et al., 1998; Tinker et al., 1996). All these reversible ryanodine derivatives exhibit lower binding affinities than ryanodine (Welch et al., 1996, 1997). Mutations D4829A and G4828A decreased the affinity and increased the dissociation rate of [^{3}H]ryanodine binding. It is possible that these mutations may also have an impact on the reversibility of ryanodine modification. To test this possibility, we examined the effect of ryanodine on single D4829A and G4828A mutant channels incorporated into planar lipid bilayers. As shown in Figs. 3 and 4, ryanodine caused single D4829A and G4828A mutant channels to enter into a long-lived open state with a reduced single channel conductance (indicated by "on" in Figs. 3 *a* and 4 *A-a*, top traces), similar to that seen with the wt RyR2 channel (indicated by "on" in Fig. 4 *B-a*, top trace). However, in the continuous presence of ryanodine and high activating Ca^{2+} concentrations, both single D4829A and G4828A mutant channels remained in the ryanodine-modified state (Figs. 3 *a* and 4 *B-a*, bottom traces). No reversal of ryanodine modification was detected under these conditions.

It has been shown that bound [^{3}H]ryanodine dissociated from RyRs faster at low Ca^{2+} concentrations than at high Ca^{2+} concentrations (Hawkes et al., 1992; Lai et al., 1989). We reasoned that we might be able to detect the reversal of ryanodine modification of the mutant channels on the time scale of single channel recordings by lowering the activating Ca^{2+} concentration. As shown in Fig. 3 *b*, upon reducing the activating Ca^{2+} concentration from 368 to 94 nM, the ryanodine-modified single D4829A mutant channel became closed in the continuous presence of ryanodine. It should be noted that this closure occurred only after reducing the Ca^{2+} concentration ($n > 10$). The closure of the ryanodine-modified D4829A mutant channel did not result from an irreversible blockade by ryanodine, because the mutant channel was reactivated upon raising the Ca^{2+} concentration to 370 nM (Fig. 3 *c*, top trace).

Interestingly, upon reactivation, normal gating events, instead of ryanodine-modified gating events, were first observed in the continuous presence of 25 μM ryanodine, then followed by an abrupt switching to the ryanodine-modified state (Fig. 3 *c*, top and bottom traces). The most likely explanation for these gating transitions is that the bound ryanodine has dissociated from the D4829A mutant channel upon lowering the activating Ca^{2+} concentration (Fig. 3 *b*). The ryanodine-unbound mutant channel was closed because the activating Ca^{2+} concentration was too low. When the Ca^{2+} concentration was increased, the ryanodine-unbound mutant channel was reactivated and was remodified shortly after its reactivation, because ryanodine was continuously present in the recording solution (Fig. 3 *c*). These transitions from normal gating state → ryanodine-modified state (in-

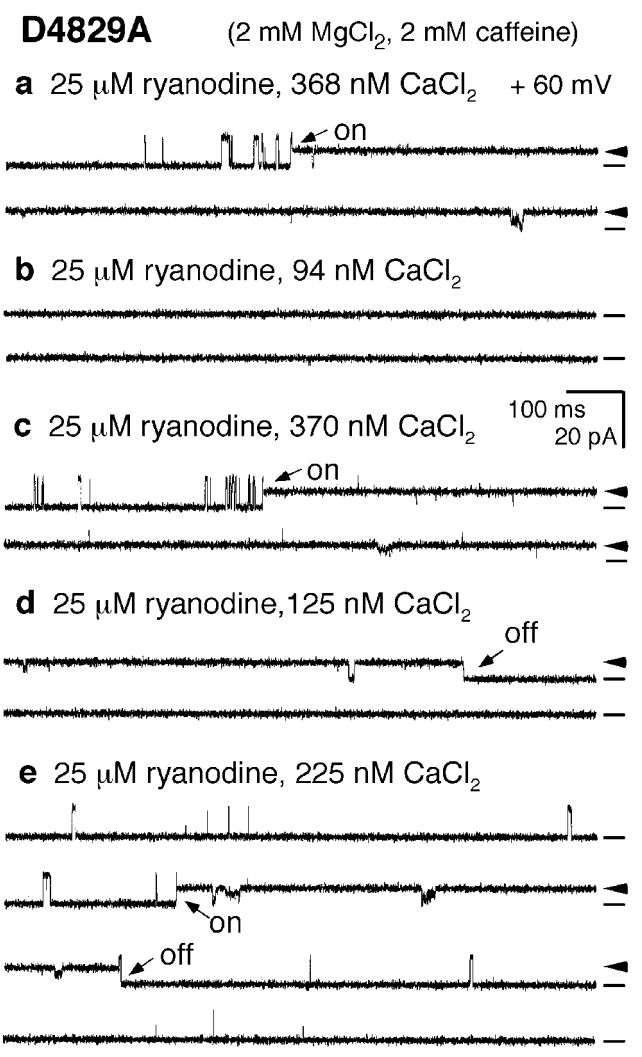

FIGURE 3 Reversible effect of ryanodine on single D4829A mutant channels. Single channel activities were recorded in a symmetrical recording solution containing 250 mM KCl and 25 mM Hepes, pH 7.4. A single D4829A mutant channel was incorporated into the bilayer with its cytoplasmic side facing the *cis* chamber, which was held at virtual ground. All additions were made to the cytoplasmic side of the channel. The D4829A channel was modified by ryanodine in the presence of 2 mM $MgCl_2$, 2 mM caffeine, and 368 nM free Ca^{2+} (*a*) at +60 mV. Openings are upward. The free Ca^{2+} was subsequently adjusted to the concentration indicated in each panel (*b–e*) by addition of an aliquot of concentrated EGTA or $CaCl_2$ solution. Gating switching from normal to ryanodine-modified (*a*), to closed state (*b*), from normal (*c*, top trace) to modified state (*c*, bottom trace), from modified to closed state (*d*), and from normal (*e*, top trace), to modified state (*e*, the second trace), and back to normal state (*e*, the third and fourth trace) are shown. Gating transitions labeled by "on" and "off" indicate the appearance and disappearance of ryanodine modification, respectively. Ryanodine, $MgCl_2$, and caffeine were present throughout the recordings. Baselines are indicated by a short line to the right of each current trace. Arrowheads show the ryanodine-modified state.

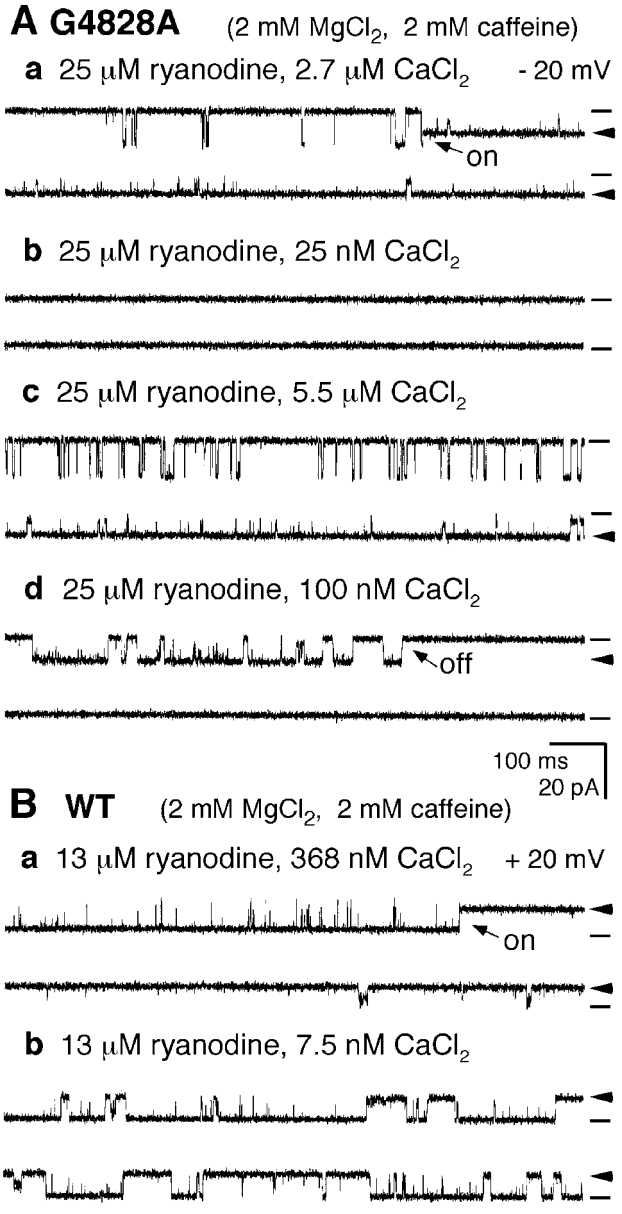

FIGURE 4 Reversible effect of ryanodine on single G4828A mutant channels. Single channel activities were recorded as described in the legend to Fig. 3. (*A*) Single G4828A mutant channel was incorporated into the bilayer with its cytoplasmic side facing the *trans* chamber, which was connected to the input of the head stage amplifier and held at −20 mV. Openings are downward. Gating switching from normal to ryanodine-modified (*a*), to closed state (*b*), from normal (*c*, top trace), to modified state (*c*, bottom trace), and from modified to closed state (*d*) are shown. (*B*) Single wt channel was modified by ryanodine (*a*) at +20 mV and remained in the modified state after reducing the Ca^{2+} concentration to 7.5 nM (*b*). Openings are upward. Ryanodine, $MgCl_2$, and caffeine were present throughout the recordings shown in *A* and *B*. Baselines are indicated by a short line to the right of each current trace. Arrowheads show the ryanodine-modified state.

dicated by "on") → closed state (indicated by "off") (Fig. 3 *d*, top trace) and back to normal gating state (Fig. 3 *e*, top trace) were repetitively observed with single D4829A mutant channels by manipulating the Ca^{2+} concentrations. Up to three such gating cycles were observed with the same single D4829A mutant channel. A direct observation of reversal of ryanodine modification of the D4829A mutant channel at the same Ca^{2+} concentration is shown in Fig. 3 *e*. At ~ 225 nM Ca^{2+} concentration, spontaneous switching between normal gating (ryanodine-unmodified state) and ryanodine-modified state (Fig. 3 *e*, the second and third trace) was observed without changing the Ca^{2+} concentration. It should be noted that in all the experiments tested for ryanodine dissociation from single D4829A mutant channels ($n = 5$), only one single channel was detected in the bilayer throughout the experiment.

Similarly, the ryanodine-modified G4828A mutant channel (Fig. 4 *A-a*, bottom trace) became closed when the activating Ca^{2+} concentration was reduced from 2.7 μM to 25 nM (Fig. 4 *A-b*) and was reactivated upon raising the Ca^{2+} concentration to 5.5 μM (Fig. 4 *A-c*, top trace). The reactivated G4828A mutant channel was modified again shortly after its reactivation by ryanodine, which was continuously present in the recording solution (Fig. 4 *A-c*, bottom trace). The ryanodine remodified G4828A mutant channel was closed again by lowering the Ca^{2+} concentration (indicated by "off" in Fig. 4 *A-d*, top trace). Such gating transitions were observed repetitively in all the single mutant G4828A channels tested ($n = 4$). Up to four such gating cycles were observed in the same single G4828A mutant channel. In contrast, under similar conditions such gating transitions were not observed with single wt channels ($n = 4$), which remained in the ryanodine-modified state after modification by ryanodine within the lifetime of the experiment (Fig. 4 *B-a*, bottom trace), even at Ca^{2+} concentrations less than 10 nM (Fig. 4 *B-b*, both traces). These results indicate that the effect of ryanodine on single D4829A and G4828A mutant channels is reversible on the time scale of single channel experiments and differs from the irreversible effect of ryanodine on single wt channels. Hence, mutations in the proposed pore-forming segment can alter the reversibility of ryanodine modification.

It should be noted that mutant D4829A exhibits a reduced single channel conductance of 160 ± 4.3 pS ($n = 5$), whereas mutant G4828A has a conductance of 757 ± 9.7 pS ($n = 4$), similar to that of the wt (~800 pS). The ryanodine-modified conductances of the wt, G4828A and D4829A mutant channels are 55.3 ± 1.8% ($n = 5$), 56.7 ± 1.0% ($n = 4$), and 55.6 ± 1.0% ($n = 5$) of their unmodified conductance, respectively. On the other hand, the ryanodine-modified conductance of the G4824A mutant channel (Zhao et al., 1999) is 80.8 ± 0.9% ($n = 6$) of its unmodified conductance. It should also be noted that both single G4828A and D4829A mutant channels are sensitive to modulation by Ca^{2+} and ryanodine (Figs. 3 and 4), and by Mg^{2+} and caffeine (data not shown). Thus, mutations in the proposed pore-forming segment can alter the conductance of both the ryanodine-modified and ryanodine-unmodified state. It is of interest to know that modifications in the

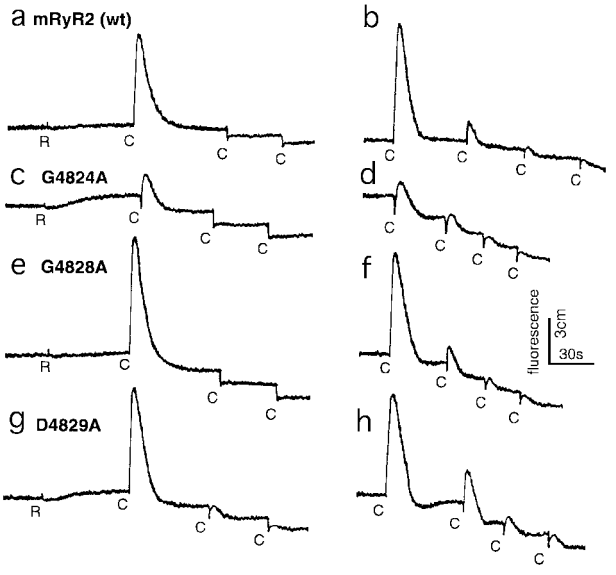

FIGURE 5 Effects of ryanodine and caffeine on intracellular Ca^{2+} release in HEK293 cells transfected with wt or mutant G4824A, G4828A, or D4829A cDNA. HEK293 cells were transfected with 6 μg of wt (*a* and *b*), G4824A (*c* and *d*), G4828A (*e* and *f*), or D4829A (*g* and *h*) cDNA. Fluorescence intensity was monitored continuously before and after addition of ryanodine (50 μM) indicated by the letter R, or caffeine (2 mM) indicated by the letter C. Decreases in fluorescence immediately after addition of caffeine were due to fluorescence quenching by caffeine. Traces shown are from a representative experiment that has been repeated three to four times. Similar results were obtained.

structure of the ryanodine molecule can also result in changes in the conductance of the ryanoid-modified state, as well as in the affinity of ryanoid binding (Welch et al., 1996, 1997).

Mutations in the proposed pore-forming segment alter the effect of ryanodine on Ca^{2+} release in HEK293 cells

To characterize the pore mutants at the whole cell level, we examined the functional effects of ryanodine and caffeine on Ca^{2+} release in HEK293 cells transfected with wt or mutant RyR2 cDNA. Fig. 5, *a* and *b* show responses to multiple caffeine stimulation of wt transfected HEK293 cells pretreated with or without ryanodine. Addition of 50 μM ryanodine to wt transfected cells did not cause significant changes in the fluorescence level (Fig. 5 *a*). Presumably most wt RyR2 channels were in a closed or in a low activity state at the resting cytoplasmic Ca^{2+} and would not be activated by ryanodine efficiently, as ryanodine interacts only with the open state of the channel. A subsequent addition of 2 mM caffeine activated the wt channel, leading to an increase in the fluorescence level (Fig. 5 *a*). However, the caffeine-activated wt channel in the presence of ryanodine failed to respond to the second or the third caffeine stimulation (Fig. 5 *a*). By contrast, in the absence of ryanodine-pretreatment, wt transfected HEK293 cells were able to respond to multiple caffeine stimulation (Fig. 5 *b*). A possible explanation for the lack of response to multiple caffeine stimulation of ryanodine-pretreated wt transfected cells is that, upon activation by caffeine in the presence of ryanodine, the wt RyR2 channel would be modified by ryanodine, and the ryanodine-modified channel would be in a fully open state and hence would no longer respond to further activation by caffeine. Alternatively, the fully activated ryanodine-modified channel would completely deplete the intracellular Ca^{2+} stores, and hence no further Ca^{2+} release could be detected by subsequent caffeine stimulation. Regardless of the exact mechanism, however, it is clear that modification of the channel by ryanodine has rendered the wt RyR2 channel unresponsive to multiple caffeine stimulation. It is noticeable that there was an immediate drop in the fluorescence level after the second or the third addition of caffeine in ryanodine-pretreated cells due to fluorescence quenching by caffeine (Chen et al., 1998; Muschol et al., 1999).

The responsiveness to multiple caffeine stimulation in the presence and absence of ryanodine can then be used as an indication for the existence of ryanodine modification. Fig. 5 shows that like the wt, mutants G4824A, G4828A, and D4829A did not respond or responded weakly to the second and third caffeine stimulation after pretreatment with ryanodine (Fig. 5, *c*, *e*, and *g*). On the other hand, in the absence of ryanodine pretreatment, Ca^{2+} release in these mutant transfected cells was observed even after the fourth caffeine stimulation (Fig. 5, *d*, *f*, and *h*). These results are consistent with our single channel data that showed that mutants G4824A, G4828A, and D4829A were modified by ryanodine (Zhao et al., 1999) (Figs. 3 and 4). The residual response of ryanodine-pretreated mutant D4829A transfected cells to the second caffeine stimulation (Fig. 5 *g*) is probably due to its low affinity and high dissociation rate of ryanodine binding (Figs. 1 and 2), which may lead to reversible ryanodine modification of the mutant channel in HEK293 cells.

The responsiveness of mutants G4820A, R4822A, and G4825A, which did not show high affinity [^{3}H]ryanodine binding, to multiple caffeine stimulation in the presence and absence of ryanodine is shown in Fig. 6. To our surprise these mutants, like wt, did not respond to the second and the third caffeine stimulation after ryanodine pretreatment (Fig. 6, *a*, *c*, and *e*), whereas they responded to multiple caffeine stimulation in the absence of ryanodine pretreatment (Fig. 6, *b*, *d*, *f*). Moreover, ryanodine alone was able to trigger a large and sustained Ca^{2+} release in mutant R4822A and mutant G4825A transfected HEK293 cells at the resting cytoplasmic Ca^{2+} before any stimulation (Fig. 6, *c* and *e*), but very little Ca^{2+} release in the wt transfected cells (Fig. 5 *a*). An intermediate level of ryanodine-induced Ca^{2+} release between those observed in the wt and in mutants R4822A and G4825A cells was also observed in mutant

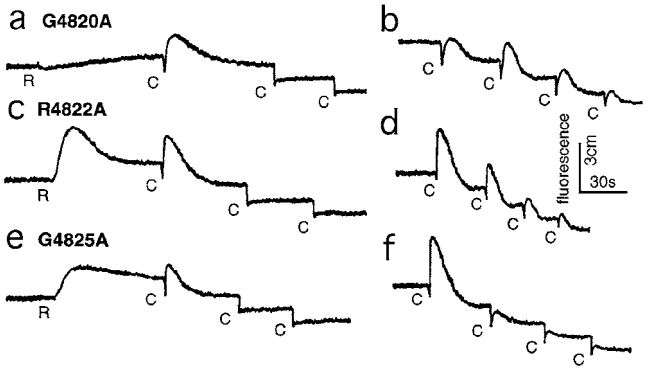

FIGURE 6 Effects of ryanodine and caffeine on intracellular Ca^{2+} release in HEK293 cells transfected with mutant G4820A, R4822A, or G4825A cDNA. HEK293 cells were transfected with 6 μg of G4820A (*a* and *b*), R4822A (*c* and *d*), or G4825A (*e* and *f*) cDNA. Fluorescence intensity was monitored continuously before and after addition of ryanodine (R, 50 μM) or caffeine (C, 2 mM). Decreases in fluorescence immediately after addition of caffeine were due to fluorescence quenching by caffeine. Traces shown are from a representative experiment that has been repeated three to four times. Similar results were obtained.

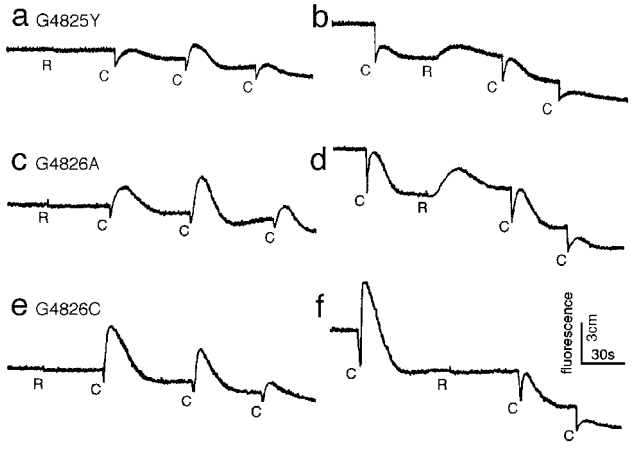

FIGURE 7 Ryanodine- and caffeine-response of mutant G4825Y, G4826A, or G4826C transfected HEK293 cells. HEK293 cells were transfected with 6 μg of G4825Y (*a* and *b*), G4826A (*c* and *d*) or G4826C (*e* and *f*) cDNA. Fluorescence was monitored continuously before and after addition of ryanodine (R, 50 μM) or caffeine (C) as described in the legend to Fig. 5. The concentration of caffeine used was 2 mM in *a*, *c*, and *e*, and 10 mM in *b*, *d*, and *f* to make sure that the lack of ryanodine response seen in *f* was not due to the low activity of the caffeine-activated mutant channel. It should also be noted that mutant G4826C after being activated by 2 mM caffeine showed no response to ryanodine either (not shown). Traces shown are from a representative experiment that has been repeated 3 to 4 times. Similar results were obtained.

G4824A (Fig. 5 *c*), mutant D4829A (Fig. 5 *g*), and mutant G4820A (Fig. 6 *a*) transfected cells. These data clearly show that mutants G4820A, R4822A, and G4825A are sensitive to ryanodine modification in HEK293 cells despite their lack of high affinity [^{3}H]ryanodine binding when determined by membrane filtration assay. These observations also indicate that mutations in the proposed pore-forming segment can influence the onset of ryanodine modification, probably by altering the accessibility of the ryanodine-binding site or the open probability of the channel at the resting cytoplasmic Ca^{2+}.

Mutations G4825Y, G4826A, and G4826C impair or eliminate the effect of ryanodine on Ca^{2+} release in HEK293 cells

Different from those observed with the wt and other mutant channels, ryanodine did not diminish Ca^{2+} release induced by the second or the third addition of caffeine in mutant G4825Y and G4826A transfected cells (Fig. 7, *a* and *c*). Furthermore, ryanodine alone was able to induce a transient Ca^{2+} release in the G4825Y and G4826A mutant transfected cells after caffeine stimulation (Fig. 7, *b* and *d*) but not before (Fig. 7, *a* and *c*). These results indicate that ryanodine can still interact with the caffeine-activated G4825Y and G4826A mutant channels despite their lack of high affinity [^{3}H]ryanodine binding. However, ryanodine did not appear to cause the G4825Y and G4826A mutant channels to enter into a fully open state, because the ryanodine-activated G4825Y and G4826A mutant channels were further activated by caffeine (Fig. 7, *a–d*). Hence, mutations in the proposed pore-forming segment can alter the characteristics of ryanodine modification, probably by affecting the gating of the ryanodine-modified state.

To further examine the role of residue G4826 in ryanodine interaction, we mutated G4826 to cysteine (G4826C) and examined the effect of ryanodine on Ca^{2+} release in G4826C transfected HEK293 cells. As shown in Fig. 7 *e*, mutant G4826C transfected cells responded to multiple caffeine stimulation in the presence of ryanodine, similar to that observed with mutant G4825Y and G4826A transfected cells (Fig. 7, *a* and *c*). However, unlike mutants G4825Y and G4826A, mutant G4826C did not respond to ryanodine either before or after caffeine stimulation (Fig. 7, *e* and *f*). The lack of ryanodine response was not due to the depletion of the Ca^{2+} stores, as further Ca^{2+} release was detected in subsequent caffeine stimulation (Fig. 7 *f*). These observations suggest that ryanodine is unable to activate or modify the G4826C mutant channel, and that residue G4826 is critical for ryanodine interaction. Therefore, a point mutation in the proposed pore-forming segment can eliminate the functional effect of ryanodine, but spares caffeine-induced Ca^{2+} release in HEK293 cells.

Co-expression of the wild-type and mutant G4826C proteins produces single channels with altered conductance and ryanodine response

Attempts to characterize the G4826C mutant at the single channel level were unsuccessful. We were unable to detect

caffeine-sensitive single G4826C mutant channels in lipid bilayers. We have previously shown that co-expression of the wt and pore mutant G4824A proteins produced hybrid channels with intermediate single channel conductances ranging between the wt conductance of 800 pS and the G4824A mutant conductance of 22 pS (Zhao et al., 1999). We reasoned that co-expression of the wt and the G4826C mutant proteins might produce hybrid channels that exhibit channel properties and ryanodine response different from those of the wt, and that these differences, if they existed, might be attributable to the mutant G4826C subunit. For these reasons, we co-transfected HEK293 cells with an equal amount of the wt and mutant G4826C cDNAs. The resulting co-expressed channels were incorporated into lipid bilayers for single channel analysis. Interestingly, we could detect only one type of hybrid channel (15 of 29) that displayed single channel conductance and gating behavior different from those of the wt (Fig. 8), and the rest of the single channels detected were similar to the wt. This was unexpected given the results of co-expression of the wt and G4824A mutant channel in which we could detect a total of four types of hybrid channels with different single channel conductances (Zhao et al., 1999). These observations imply that some hybrid channels, like the G4826C mutant channel, may not be detectable in lipid bilayers.

As shown in Fig. 8, a single wt/G4826C hybrid channel exhibited two major substates (~3/4 and ~1/4) and resided mostly in the ~3/4 substate with brief transitions from the ~3/4 substate to the fully open state (Fig. 8 *a*). Transitions from the closed state to the fully open state were also observed (indicated by asterisks) (Fig. 8 *a*). The fully open state of the wt/G4826C hybrid channel exhibited a unitary conductance of 1000–1100 pS. The exact subunit composition of the hybrid channel is not clear. The detection of only one type of hybrid channels and the appearance of ~3/4 and ~1/4 substates seem to favor the stoichiometry of three wt subunits and one G4826C mutant subunit. The wt/G4826C hybrid channel appeared to be partially sensitive to ryanodine modification. Whereas the ~3/4 substate was shifted by ryanodine into a long-lived open state with brief closings and reduced conductance, the ~1/4 substate was not converted to fully open state and remained flickering with variable conductances upon ryanodine modification (Fig. 8, *b–d*). Furthermore, the wt/G4826C hybrid channel displayed multiple ryanodine-modified states and switched between these states spontaneously (indicated by arrows in Fig. 8 *c*). It is of interest to know that two ryanoid-modified states were also detected with some ryanodine derivatives, for example, 8β-amino-9α-hydroxyryanodine (Williams et al., 2000). In addition, the effect of ryanodine on single wt/G4826C hybrid channels was reversible, similar to that seen with single G4828A and D4829A mutant channels (Figs. 3 and 4). Gating transitions from the ryanodine-modified state to the closed state (indicated by "off" in Fig. 8 *c*), to the normal gating state (ryanodine-unmodified state) (Fig. 8 *d*), and to the ryanodine modified state (indicated by "on" in Fig. 8 *d*) were observed repetitively in the continuous presence of ryanodine by changing the Ca^{2+} concentrations (Fig. 8 *e*) ($n = 5$). These observations indicate that mutation G4826C introduced into one (or more) subunit(s) of the tetrameric RyR channel can alter the single channel conductance, the reversibility of ryanodine modification, and the conductance, gating, and stability of the ryanodine-modified state, consistent with the essential role of this residue in ryanodine interaction.

DISCUSSION

In this study we have demonstrated for the first time that mutations in the proposed pore-forming segment of RyR can 1) increase or decrease the dissociation rate of [^{3}H]ryanodine binding, 2) change the reversibility of ryanodine modification at the single channel level, 3) eliminate the functional effect of ryanodine on Ca^{2+} release in HEK293 cells without abolishing caffeine response, and 4) alter the conductance, stability, and gating behavior of the ryanodine-modified state. These observations strongly suggest that the proposed pore-forming segment is an essential determinant of ryanodine-RyR interaction. It is of interest to note that structural modifications of the ryanodine molecule also affect the affinity of ryanoid binding, the reversibility of ryanoid modification of the RyR channel, and the conductance and gating of the ryanoid-modified state (Sutko et al., 1997; Tanna et al., 1998; Tinker et al., 1996; Welch et al., 1996, 1997). In other words, the effects on ryanodine-RyR interaction of mutations in the proposed pore-forming segment mirror those induced by changing the structure of the ryanodine molecule.

Determinants of ryanodine interaction in the ryanodine molecule

The structural determinants in the ryanodine molecule that are essential for ryanodine-RyR interaction have been investigated by using comparative molecular field analysis of a number of ryanodine derivatives. These studies demonstrate that the pyrrole group of the ryanodine molecule is absolutely required for high affinity ryanodine binding. Small modifications introduced into the pyrrole group at the 3-position of the ryanodine molecule led to a dramatic reduction in binding affinity. In contrast, additions of large, bulky or charged groups at the 9 or 10 position of ryanodine caused only minor changes in binding properties (Sutko et al., 1997; Welch et al., 1994, 1996, 1997). These observations have led to the suggestion that the pyrrole group at one end of the ryanodine molecule would interact with a specific and hydrophobic crevice on RyR, whereas the other end of the ryanodine molecule (the 9 and 10 positions) would be

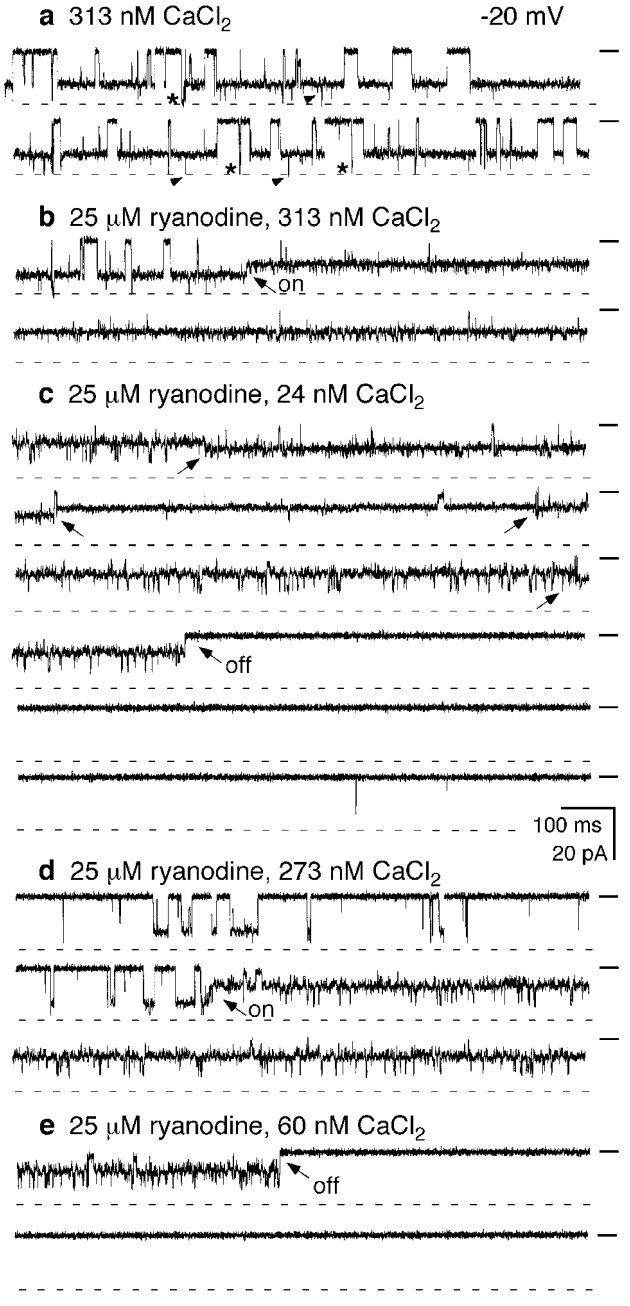

FIGURE 8 Single hybrid channels formed by wt and mutant G4826C proteins display altered conductance and ryanodine response. Single channel currents were recorded in a symmetrical recording solution containing 250 mM KCl and 25 mM Hepes, pH 7.4. (*a*) Single wt/G4826C hybrid channel was incorporated into the bilayer with its cytoplasmic side facing the *trans* chamber, which was connected to the input of the head stage amplifier and was held at −20 mV. Openings are downward. All additions were made to the cytoplasmic side of the channel. The hybrid channel was modified by ryanodine (25 μM) in the presence of 313 nM free Ca^{2+} (*b*). The free Ca^{2+} was subsequently adjusted to the concentration indicated in each panel (*c–e*) by addition of an aliquot of concentrated EGTA or $CaCl_2$ solution. Gating transitions labeled by "on" and "off" indicate the appearance and disappearance of ryanodine-modified state, respectively. Arrows show switching between different ryanodine-modified states. Dash lines and asterisks indicate the fully open state and arrowheads show the ~1/4 substate. Ryanodine (25 μM) was present throughout the recordings shown in *b* through *e*. Baselines are indicated by a short line to the right of each current trace.

situated at the mouth or outside of the binding site, which would be in contact with the solvent (Sutko et al., 1997; Welch et al., 1996). In addition to the pyrrole group, hydrophobic and electrostatic interactions are believed to be involved in ryanodine-RyR interaction as well. In this context, it is of interest to note that the ryanodine molecule possesses a unique pattern of distribution of hydrophobic and polar fields: one side of the molecule is mainly hydrophobic, whereas the other is largely polar (Welch et al., 1994).

Structural features of the RyR conduction pathway

It is apparent from mutational studies, previous functional studies, and comparative molecular field analysis that ryanodine is likely to bind to a site within the conduction pathway of RyR (Tanna et al., 1998, 2000; Tinker et al., 1996). However, the exact location of the ryanodine binding site and the structure of the RyR conduction pathway are unknown. Permeation studies of a variety of permeant and impermeant inorganic and organic cations revealed the presence of several basic structural features in the RyR ion conduction pathway. These include a short selectivity filter, a hydrophobic cation-binding site near the selectivity filter, a hydrophilic cation-binding site, and a large vestibule. The large vestibule is thought to locate in the cytoplasmic mouth of the channel, whereas the narrow selectivity filter is believed to locate at ~90% into the ~10 Å voltage drop from the cytoplasmic side and has a diameter of ~7 Å (Lindsay et al., 1994).

A more detailed model of the RyR conduction pathway has been proposed recently (Williams et al., 2001) based on the results of site-directed mutagenesis on the proposed pore-forming segment, previous biophysical studies of the conduction pathway, and the three-dimensional structure of the bacterial potassium channel, KcsA (Doyle et al., 1998). In this model, the predicted transmembrane segment TM8, the putative pore helix, the putative selectivity filter, and the predicted transmembrane segment TM10 of RyR (Fig. 9 *a*) (Zorzato et al., 1990) were proposed to correspond to the outer helix, the pore helix, the signature sequence, and the inner helix of KcsA channel, respectively, and to arrange in the membrane in a manner similar to that found in the KcsA channel (Williams et al., 2001) (Fig. 9 *b*). Compared with the KcsA channel, however, the hypothetical selective filter of the RyR conduction pathway would be much larger in diameter (~3 Å in KcsA vs. ~7 Å in RyR). The narrowest region of the RyR pore has been estimated to be less than 1 Å in length. The selectivity filter would be located close to the luminal end of the channel. It was also proposed that the hypothetical RyR pore as in the KcsA channel would have a large cavity located in the lipid membrane and an inner pore with a large capture radius at the cytoplasmic end (Fig. 9 *b*).

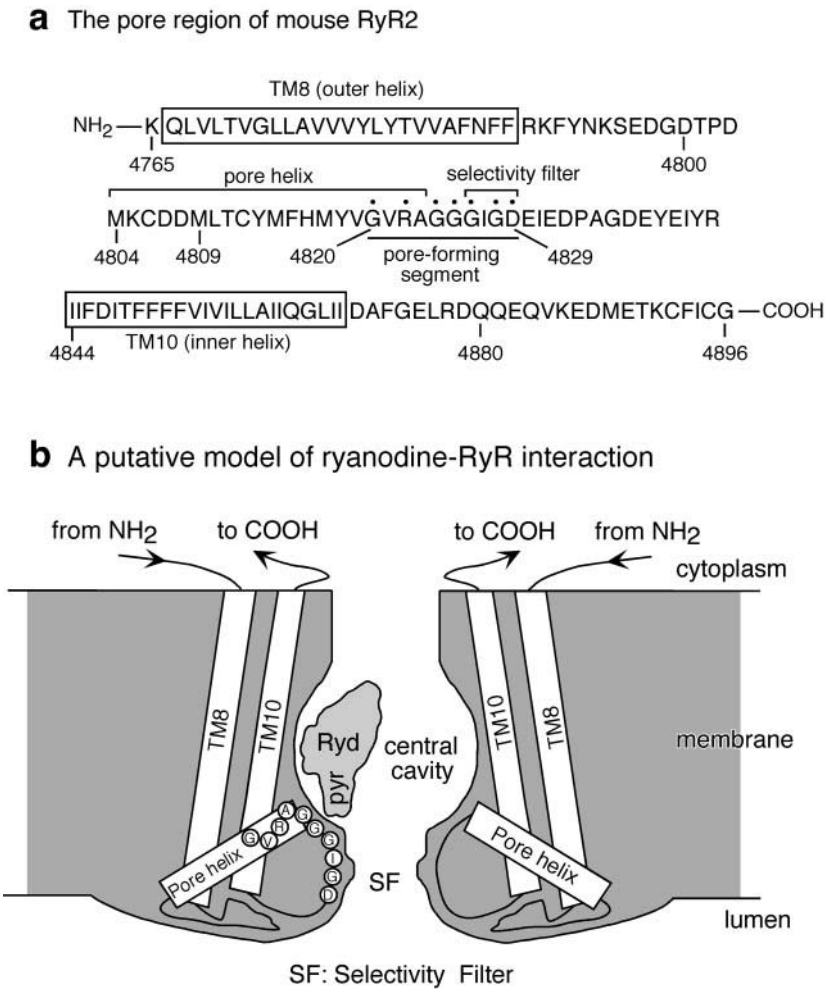

FIGURE 9 Cartoon illustrating the interactions between ryanodine and the RyR conduction pathway. (*a*) Amino acid sequence in single letter codes of the pore region of mouse RyR2. The predicted transmembrane segments, TM8 and TM10, according to the transmembrane model of Zorzato et al. (1990), the predicted pore helix and selectivity filter (Williams et al., 2001), and the proposed pore forming segment (Zhao et al., 1999) are indicated. Numbers indicate the amino acid positions. The sequences of TM8 and TM10 are thought to correspond to the outer helix and inner helix of the KcsA channel, respectively (Williams et al., 2001). (●) Residues that were mutated and characterized in this study. (*b*) Hypothetical model for ryanodine-RyR interactions. The model shown for the RyR conduction pathway was adopted from that proposed by Williams et al. (2001) with some modifications. (□) Depict TM8 (outer helix), TM10 (inner helix), and the putative pore helix connected together by two loops and arranged in a manner similar to that found in the KcsA channel. The putative central cavity and the putative selectivity filter (SF) are indicated. Only part of the transmembrane assembly of RyR near the conduction pathway from two RyR monomers is shown. The cytoplasmic assembly or the "foot" domain of RyR and the stalk between the cytoplasmic assembly and the lipid membrane are omitted in the model. The entire transmembrane assembly has an estimated dimension of ~120 × 120 × 65 Å (Orlova et al., 1996; Sharma et al., 1998). We propose that ryanodine (Ryd) binds to the putative central cavity of the RyR conduction pathway with its pyrrole group (pyr) anchoring at a specific site near the selectivity filter (SF) and its opposite end pointing toward the cytoplasmic mouth of the conduction pathway. The estimated dimensions of the ryanodine molecule and the putative selectivity filter were drawn to scale relative to the membrane bilayer.

The central cavity in the KcsA channel is believed to play an essential role in ion selectivity and ion translocation (Doyle et al., 1998). It has recently been shown that the central cavity and inner pore also form the binding site for the inactivation gate and potassium channel blocking cations such as tetrabutylammonium (Zhou et al., 2001). Interestingly, the potassium channel N-type inactivation peptide, tetrabutylammonium, and many other tetraalkylamonium ions have been shown to be able to block also the RyR channel (Mead et al., 1998; Tinker et al., 1992; Williams et al., 2001). These observations indicate that the RyR conduction pathway also contain a receptor site, probably corresponding to the putative central cavity in RyR, for these potassium channel blocking cations and peptides.

Hypothetical model for ryanodine-RyR interactions

Mutational studies have suggested that the proposed pore-forming segment plays an essential role in ion conduction and permeation, and is likely to constitute part of the selectivity filter, as indicated in the RyR pore model of Williams et al. (2001). To incorporate the results of this study that the proposed pore-forming segment is an essential determinant of ryanodine interaction, we hypothesize that ryanodine most likely binds to the putative central cavity of the RyR conduction pathway with its pyrrole group interacting, in part, with part of the proposed pore-forming segment (Fig. 9 *b*). More specifically, in this hypothetical model, the proposed pore-forming segment would contribute to the formation of part of the putative selectivity filter and part of the putative pore helix. Residues in the putative pore helix are believed to interact with residues in the putative selectivity filter to stabilize the structure, as seen in the three-dimensional structure of the KcsA channel (Doyle et al., 1998). The pyrrole group of the ryanodine molecule would bind to a unique and specific site in the central cavity adjacent to the putative selectivity filter, whereas the opposite end of the ryanodine molecule would point to the cytoplasmic mouth of the channel. Furthermore, the hydrophobic hemisphere of the ryanodine molecule would interact with the hydrophobic inner wall of the putative central cavity, and the polar side would face the aqueous pore in contact with the solvent. Thus, in addition to the proposed

pore-forming segment, other regions of the conduction pathway including the TM10 or TM8 sequence may also be involved in ryanodine binding. The putative central cavity in RyR would be large enough to hold a ryanodine molecule, which has an estimated dimension of 16 × 9 × 8 Å (W. Welch, personal communication), without being plugged by ryanodine completely. Moreover, each RyR monomer would have a potential ryanodine-binding site based on the negatively cooperative mechanism of ryanodine binding (Lai et al., 1989; McGrew et al., 1989; Pessah and Zimanyi, 1991).

According to this hypothetical model, binding of ryanodine would be expected to affect the conformation of the selectivity filter and the inner conduction pore. These effects would be expected to result in the observed changes in ion handling, single channel conductance, and gating upon ryanodine binding. On the other hand, mutations in the proposed pore-forming segment would be expected to affect ryanodine binding directly or indirectly by altering the interactions between the putative pore helix and the putative selectivity filter, thus the conformation of the selectivity filter region that is involved in ryanodine binding. Such an orientation of ryanodine binding within the putative central cavity would be also in agreement with the observations that the pyrrole group of the ryanodine molecule has a primary role in its binding and modulation of RyR channel function, whereas the opposite pole of the molecule has only a minor effect. Thus, this hypothetical model is apparently consistent with the results of mutational studies and comparative molecule field analysis. The RyR pore is believed to have a much larger diameter than that of the KcsA channel. Hence, in addition to TM8, TM10, the putative pore helix, and the putative selectivity filter, other transmembrane segments may contribute to the formation of the RyR pore. This hypothetical working model would provide a useful framework for further investigation of the molecular mechanisms of ryanodine action and ion conduction of the RyR channel.

We thank Drs. Alan J. Williams, William Welch, John L. Sutko, and Jonathan Lytton for helpful discussions, Robert J. Winkfein for the synthesis of DNA primers, Dr. Wayne R. Giles and the Ion Channels and Transporters Group for continuous support, Dr. Paul M. Schnetkamp for the use of his luminescence spectrometer, and Jeff Bolstad for critical reading of the manuscript.

This work was supported by research grants from the Canadian Institutes of Health Research and the Heart and Stroke Foundation of Alberta, N.W.T., and Nunavut to S.R.W.C.

REFERENCES

Berridge, M. J. 1993. Inositol trisphosphate and calcium signaling. *Nature.* 361:315–325.

Bhat, M. B., J. Zhao, H. Takeshima, and J. Ma. 1997. Functional calcium release channel formed by the carboxyl-terminal portion of ryanodine receptor. *Biophys. J.* 73:1329–1336.

Callaway, C., A. Seryshev, J. P. Wang, K. J. Slavik, D. H. Needleman, C. Cantu, 3rd, Y. Wu, T. Jayaraman, A.R. Marks, and S.L. Hamilton. 1994. Localization of the high and low affinity [3H]ryanodine binding sites on the skeletal muscle Ca2+ release channel. *J. Biol. Chem.* 269: 15876–15884.

Chen, S. R., K. Ebisawa, X. Li, and L. Zhang. 1998. Molecular identification of the ryanodine receptor Ca2+ sensor. *J. Biol. Chem.* 273: 14675–14678.

Chen, S. R. W., P. Li, M. Zhao, X. Li, and L. Zhang. 2000. The ryanodine receptor pore-forming segment constitutes an essential part of the ryanodine binding site. *Biophys. J.* 78:149A.

Clapham, D. E. 1995. Calcium signaling. *Cell.* 80:259–268.

Coronado, R., J. Morrissette, M. Sukhareva, and D. M. Vaughan. 1994. Structure and function of ryanodine receptors. *Am. J. Physiol.* 266: C1485–C1504.

Doyle, D. A., J. Morais Cabral, R. A. Pfuetzner, A. Kuo, J. M. Gulbis, S. L. Cohen, B. T. Chait, R. MacKinnon, A. Norris, D. M. Geddes, and A. J. Williams. 1998. The structure of the potassium channel: molecular basis of K+ conduction and selectivity. *Science.* 280:69–77.

Du, G. G., X. Guo, V. K. Khanna, and D. H. MacLennan. 2001. Functional characterization of mutants in the predicted pore region of the rabbit cardiac muscle Ca(2+) release channel (ryanodine receptor isoform 2). *J. Biol. Chem.* 276:31760–31771.

Fabiato, A., and F. Fabiato. 1979. Calculator programs for computing the composition of the solutions containing multiple metals and ligands used for experiments in skinned muscle cells. *J. Physiol. (Paris).* 75:463–505.

Franzini-Armstrong, C., and F. Protasi. 1997. Ryanodine receptors of striated muscles: a complex channel capable of multiple interactions. *Physiol. Rev.* 77:699–729.

Gao, L., D. Balshaw, L. Xu, A. Tripathy, C. Xin, and G. Meissner. 2000. Evidence for a role of the lumenal M3–M4 loop in skeletal muscle Ca(2+) release channel (Ryanodine receptor) activity and conductance [In Process Citation]. *Biophys. J.* 79:828–840.

Hawkes, M. J., T. E. Nelson, and S. L. Hamilton. 1992. [3H]ryanodine as a probe of changes in the functional state of the Ca(2+)-release channel in malignant hyperthermia. *J. Biol. Chem.* 267:6702–6709.

Ho, S. N., H. D. Hunt, R. M. Horton, J. K. Pullen, and L. R. Pease. 1989. Site-directed mutagenesis by overlap extension using the polymerase chain reaction. *Gene.* 77:51–59.

Lai, F. A., M. Misra, L. Xu, H. A. Smith, and G. Meissner. 1989. The ryanodine receptor-Ca2+ release channel complex of skeletal muscle sarcoplasmic reticulum: evidence for a cooperatively coupled, negatively charged homotetramer. *J. Biol. Chem.* 264:16776–16785.

Li, P., and S. R. Chen. 2001. Molecular basis of ca(2)+ activation of the mouse cardiac ca(2)+ release channel (ryanodine receptor). *J. Gen. Physiol.* 118:33–44.

Lindsay, A. R., A. Tinker, and A. J. Williams. 1994. How does ryanodine modify ion handling in the sheep cardiac sarcoplasmic reticulum Ca(2+)-release channel? *J. Gen. Physiol.* 104:425–447.

McGrew, S. G., C. Wolleben, P. Siegl, M. Inui, and S. Fleischer. 1989. Positive cooperativity of ryanodine binding to the calcium release channel of sarcoplasmic reticulum from heart and skeletal muscle. *Biochemistry.* 28:1686–1691.

Mead, F. C., D. Sullivan, and A. J. Williams. 1998. Evidence for negative charge in the conduction pathway of the cardiac ryanodine receptor channel provided by the interaction of K+ channel N-type inactivation peptides. *J. Membr. Biol.* 163:225–234.

Meissner, G. 1994. Ryanodine receptor/Ca2+ release channels and their regulation by endogenous effectors. *Annu. Rev. Physiol.* 56:485–508.

Muschol, M., B. R. Dasgupta, and B. M. Salzberg. 1999. Caffeine interaction with fluorescent calcium indicator dyes. *Biophys. J.* 77:577–586.

Ogawa, Y. 1994. Role of ryanodine receptors. *Crit. Rev. Biochem. Mol. Biol.* 29:229–274.

Orlova, E. V., Serysheva, I. I., M. van Heel, S. L. Hamilton, and W. Chiu. 1996. Two structural configurations of the skeletal muscle calcium release channel. *Nat. Struct. Biol.* 3:547–552.

Pessah, I. N., and I. Zimanyi. 1991. Characterization of multiple [3H]ryanodine binding sites on the Ca2+ release channel of sarcoplasmic

reticulum from skeletal and cardiac muscle: evidence for a sequential mechanism in ryanodine action. *Mol. Pharmacol.* 39:679–689.

Sharma, M. R., P. Penczek, R. Grassucci, H. B. Xin, S. Fleischer, and T. Wagenknecht. 1998. Cryoelectron microscopy and image analysis of the cardiac ryanodine receptor. *J. Biol. Chem.* 273:18429–18434.

Sutko, J. L., J. A. Airey, W. Welch, and L. Ruest. 1997. The pharmacology of ryanodine and related compounds. *Pharmacol. Rev.* 49:53–98.

Tanna, B., W. Welch, L. Ruest, J. L. Sutko, and A. J. Williams. 1998. Interactions of a reversible ryanoid (21-amino-9alpha-hydroxy-ryanodine) with single sheep cardiac ryanodine receptor channels. *J. Gen. Physiol.* 112:55–69.

Tanna, B., W. Welch, L. Ruest, J. L. Sutko, and A. J. Williams. 2000. The interaction of a neutral ryanoid with the ryanodine receptor channel provides insights into the mechanisms by which ryanoid binding is modulated by voltage. *J. Gen. Physiol.* 116:1–9.

Tinker, A., A. R. Lindsay, and A. J. Williams. 1992. Large tetraalkyl ammonium cations produce a reduced conductance state in the sheep cardiac sarcoplasmic reticulum Ca(2+)-release channel. *Biophys. J.* 61:1122–1132.

Tinker, A., J. L. Sutko, L. Ruest, P. Deslongchamps, W. Welch, J. A. Airey, K. Gerzon, K. R. Bidasee, H. R. Besch, Jr., and A. J. Williams. 1996. Electrophysiological effects of ryanodine derivatives on the sheep cardiac sarcoplasmic reticulum calcium-release channel. *Biophys. J.* 70:2110–2119.

Weiland, G. A., and P. B. Molinoff. 1981. Quantitative analysis of drug-receptor interactions: I. Determination of kinetic and equilibrium properties. *Life Sci.* 29:313–330.

Welch, W., S. Ahmad, J. A. Airey, K. Gerzon, R. A. Humerickhouse, H. R. Besch, Jr., L. Ruest, P. Deslongchamps, and J. L. Sutko. 1994. Structural determinants of high-affinity binding of ryanoids to the vertebrate skeletal muscle ryanodine receptor: a comparative molecular field analysis. *Biochemistry.* 33:6074–6085.

Welch, W., J. L. Sutko, K. E. Mitchell, J. Airey, and L. Ruest. 1996. The pyrrole locus is the major orienting factor in ryanodine binding. *Biochemistry.* 35:7165–7173.

Welch, W., A. J. Williams, A. Tinker, K. E. Mitchell, P. Deslongchamps, J. Lamothe, K. Gerzon, K. R. Bidasee, H. R. Besch, Jr., J. A. Airey, J. L. Sutko, and L. Ruest. 1997. Structural components of ryanodine responsible for modulation of sarcoplasmic reticulum calcium channel function. *Biochemistry.* 36:2939–2950.

Williams, A. J., N. Haji, B. Tanna, W. Welch, L. Ruest, and J. Sutko. 2000. Excess noise in the ryanoid-modified conductance state of the RyR2 channel. *Biophys. J.* 78:A191.

Williams, A. J., D. J. West, and R. Sitsapesan. 2001. Light at the end of the Ca(2+)-release channel tunnel: structures and mechanisms involved in ion translocation in ryanodine receptor channels. *Q. Rev. Biophys.* 34: 61–104.

Witcher, D. R., P. S. McPherson, S. D. Kahl, T. Lewis, P. Bentley, M. J. Mullinnix, J. D. Windass, and K. P. Campbell. 1994. Photoaffinity labeling of the ryanodine receptor/Ca2+ release channel with an azido derivative of ryanodine. *J. Biol. Chem.* 269:13076–13079.

Zhao, M., P. Li, X. Li, L. Zhang, R. J. Winkfein, and S. R. Chen. 1999. Molecular identification of the ryanodine receptor pore-forming segment. *J. Biol. Chem.* 274:25971–25974.

Zhou, M., J. H. Morais-Cabral, S. Mann, R. MacKinnon, M. Muschol, B. R. Dasgupta, and B. M. Salzberg. 2001. Potassium channel receptor site for the inactivation gate and quaternary amine inhibitors. *Nature.* 411:657–661.

Zorzato, F., J. Fujii, K. Otsu, M. Phillips, N. M. Green, F. A. Lai, G. Meissner, and D. H. MacLennan. 1990. Molecular cloning of cDNA encoding human and rabbit forms of the Ca2+ release channel (ryanodine receptor) of skeletal muscle sarcoplasmic reticulum. *J. Biol. Chem.* 265:2244–2256.